

Impact of different interaction behavior on epidemic spreading in time-dependent social networks

Shuai Huang(黄帅), Jie Chen(陈杰), Meng-Yu Li(李梦玉), Yuan-Hao Xu(徐元昊), and Mao-Bin Hu(胡茂彬)

Citation: Chin. Phys. B, 2024, 33 (**3**): 030205. DOI: 10.1088/1674-1056/ad147f
Journal homepage: http://cpb.iphy.ac.cn; http://iopscience.iop.org/cpb

What follows is a list of articles you may be interested in

Effect of conformity on evolution of cooperation in a coordination game

Xianjia Wang(王先甲) and Tao Wang(王饕)
Chin. Phys. B, 2023, 32 (**10**): 100202. DOI: 10.1088/1674-1056/acd9c2

Intervention against information diffusion in static and temporal coupling networks

Yun Chai(柴允), You-Guo Wang(王友国), Jun Yan(颜俊), and Xian-Li Sun(孙先莉)
Chin. Phys. B, 2023, 32 (**9**): 090202. DOI: 10.1088/1674-1056/acb9f4

Robustness measurement of scale-free networks based on motif entropy

Yun-Yun Yang(杨云云), Biao Feng(冯彪), Liao Zhang(张辽), Shu-Hong Xue(薛舒红), Xin-Lin Xie(谢新林), and Jian-Rong Wang(王建荣)
Chin. Phys. B, 2022, 31 (**8**): 080201. DOI: 10.1088/1674-1056/ac6942

Effect of observation time on source identification of diffusion in complex networks

Chaoyi Shi(史朝义), Qi Zhang(张琦), and Tianguang Chu(楚天广)
Chin. Phys. B, 2022, 31 (**7**): 070203. DOI: 10.1088/1674-1056/ac5985

Dynamics and intermittent stochastic stabilization of a rumor spreading model with guidance mechanism in heterogeneous network

Xiaojing Zhong(钟晓静), Yukun Yang(杨宇琨), Runqing Miao(苗润青), Yuqing Peng(彭雨晴), and Guiyun Liu(刘贵云)
Chin. Phys. B, 2022, 31 (**4**): 040205. DOI: 10.1088/1674-1056/ac587d

---

Impact of different interaction behavior on epidemic spreading in time-dependent social networks

Shuai Huang(黄帅)[1], Jie Chen(陈杰)[2], Meng-Yu Li(李梦玉)[1], Yuan-Hao Xu(徐元昊)[1], and Mao-Bin Hu(胡茂彬)[1,†]

[1] *School of Engineering Science, University of Science and Technology of China, Hefei* 230026, *China*
[2] *School of Mathematics, Southeast University, Nanjing* 210096, *China*

(Received 12 September 2023; revised manuscript received 17 November 2023; accepted manuscript online 12 December 2023)

We investigate the impact of pairwise and group interactions on the spread of epidemics through an activity-driven model based on time-dependent networks. The effects of pairwise/group interaction proportion and pairwise/group interaction intensity are explored by extensive simulation and theoretical analysis. It is demonstrated that altering the group interaction proportion can either hinder or enhance the spread of epidemics, depending on the relative social intensity of group and pairwise interactions. As the group interaction proportion decreases, the impact of reducing group social intensity diminishes. The ratio of group and pairwise social intensity can affect the effect of group interaction proportion on the scale of infection. A weak heterogeneous activity distribution can raise the epidemic threshold, and reduce the scale of infection. These results benefit the design of epidemic control strategy.

Keywords: epidemic transmission, complex network, time-dependent networks, social interaction

PACS: 02.70.Uu, 02.60.Cb, 05.10.–a, 05.10.Ln **DOI:** 10.1088/1674-1056/ad147f

1. Introduction

The outbreak of epidemics poses a significant threat to human society, emphasizing the crucial need to develop effective epidemic-control strategies.[1–3] The emergence of complex network theory provided a novel framework for better comprehension of various propagation problems, including epidemics, rumor, ideas, and cyber viruses.[4–7] Compartment models including susceptible–infected (SI), susceptible–infected–susceptible (SIS), and susceptible–infected–recovered (SIR) models have been extensively investigated to provide insights on how to mitigate spreading. However, most studies in literature assume that individual interactions are static,[8,9] potentially leading to erroneous conclusions.[10] Indeed, interactions between individuals have strong time-dependent and evolving properties, which can be effectively captured by temporal or activity-driven (AD) networks.[11] In the AD network, each node has an activity potential, representing the probability of being activated. Wang *et al.*[12] utilized the AD network to investigate the effects of individual behaviors on epidemics. Hou *et al.*[13] analyzed the impact of social attitudes on the spread of epidemics.

In research of epidemic transmission patterns in social networks, various methods for intelligent analysis of social network images have been proposed to extract relevant information from social networks. For instance, Li *et al.* introduced the weakly supervised deep matrix factorization (WDMF) algorithm, which effectively addresses issues related to social image label refinement, label assignment, and image retrieval by revealing latent representations of images and labels.[14] Subsequently, Li *et al.* also proposed a model called deep collaborative embedding (DCE) to achieve knowledge from images contributed by the community and leverage weakly supervised contextual information for multiple image understanding tasks.[15] This model adopts a unified framework that combines end-to-end learning and collaborative factor analysis to optimize representation learning and explore latent spaces.

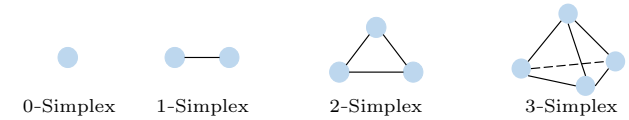


Fig. 1. The structures of $(s-1)$-simplex ($s = 1$, 2, 3, and 4) and simplex complex. Here $(s-1)$-simplex is a $(s-1)$-dimensional polyhedron, which is a convex hull composed of its $s-1$ vertices (nodes).

Most studies modeled individual interaction as pairwise links, while neglecting the effects of group interaction on epidemics. In social networks, the simultaneous sharing of false information by multiple individuals increases the likelihood of it being believed.[16] In collaborations among scientists, group connections are common involving multiple authors working on a scientific paper.[17] Therefore, networks with higher-order interactions describing group dynamics have emerged as powerful framework for modeling collective behaviors, including simplicial complexes and hypergraphs.[18] As shown in Fig. 1, a simplicial complex K is a set of simplexes that

†Corresponding author. E-mail: humaobin@ustc.edu.cn

© 2024 Chinese Physical Society and IOP Publishing Ltd

satisfy the following conditions: (i) all proper subfaces of the simplex s are also in s; (ii) the intersection of any two simplexes $\sigma_1 \in s$ and $\sigma_2 \in s$[19–21] is a common face of $\sigma_1 \in s$ and $\sigma_2 \in s$. Based on this concept, Petri *et al.* introduced a simplicial activity-driven (SAD) model and demonstrated that the structure of the simplicial complex influences the contagion process.[22] In the SAD model, nodes activated at each time step randomly choose $(s-1)$ other nodes to form a simplex, where a $(s-1)$-simplex is defined as a set of s vertices.

During the COVID-19 pandemic, there exist diverse social interactions in response to government measures, including pairwise and group interactions.[23–25] However, the effects of different social interactions on the spread of epidemics in time-dependent networks are still not well understood. To fill this gap, this paper presents a comprehensive model that integrates both pairwise and group interactions. In this model, group interactions are modeled by simplicial structures, while pairwise interactions are represented by pairwise links. A parameter p is introduced to control the pairwise interaction proportion in the network (i.e., $1-p$ is the proportion of group interaction). Meanwhile, the parameter $(s-1)$ represents the group social intensity, and the parameter of m (links to other individuals) represents the pairwise social intensity. By extensive simulation and theoretical analysis, the effects of pairwise/group interaction proportions, and pairwise/group interaction intensities are widely explored. It is found that an increase in the pairwise interaction proportion can effectively mitigate the spread of the epidemic under the condition that the group social intensity equals the pairwise social intensity. Reducing the group social intensity can slow down the epidemic spreading when the pairwise interaction proportion is low. However, as the pairwise interaction proportion increases, the epidemic suppressing effect of reducing group social intensity becomes less significant. Interestingly, with high group social intensity (larger than or equal to pairwise social intensity), increasing the pairwise interaction proportion leads to a decrease in the scale of infection. Conversely, when group social intensity is low (less than pairwise social intensity), increasing the proportion of pairwise interactions results in larger scale of infection. Additionally, a weak heterogeneous activity distribution raises the epidemic threshold while reduces the scale of infection. These results can benefit the design of epidemic control strategies.

The paper is structured as follows: In Section 2 we introduce the epidemic model. In Section 3, we analyze the impact of pairwise/group interaction proportions, the pairwise/group interaction intensities, and heterogeneous activity distribution on the epidemic threshold. Finally, in Section 4 we summarize the main findings.

2. Model

This section introduces our model of activity-spreading network with multiple modes of social interactions.

2.1. Activity-driven network with pairwise/group interactions

In this time-varying network, N nodes are characterized by an activity distribution $F(a)$, from which the activity $a_{i=1,2,\ldots,N}$ of each node i are extracted.[11] The activity a_i represents the firing probability of node i and is fixed throughout the whole process. Its probability distribution is $F(a) \propto a^{-\gamma_a}$, where $2 < \gamma_a < 3$ and $\varepsilon \leqslant a \leqslant 1$, to avoid divergence.

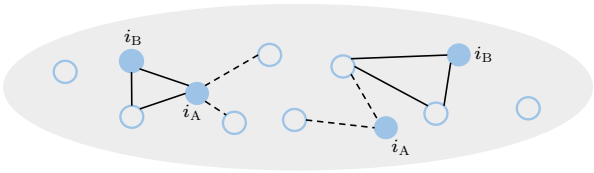


Fig. 2. Schematic illustration of time-varying network of populations with different social interactions. Here the blue solid nodes represent active nodes.

For the simplicity of mean field analysis, we assume that group interactions involve individuals who do not participate pairwise social interactions. Similarly, individuals engaged in pairwise social interactions will not participate in group activities. Individuals are classified into two types based on their social interaction patterns during epidemic outbreak. Each individual is randomly assigned to one of the two types (A or B). Type-A individuals engage in pairwise interactions, while type-B individuals engage in group interactions. The pairwise interaction proportion is denoted by p, indicating that pN individuals out of the total population of N engage in pairwise interactions. The remaining $(1-p)N$ individuals engage in group interactions.

At each time step, each node i fires with probability of $a_i\Delta t$. If node i belongs to type A, it connects m nodes randomly; on the contrary, if node i belongs to type B, it selects $(s-1)$ nodes uniformly at random to form a $(s-1)$-simplex, where s represents the social intensity of node i. The parameter $(s-1)$ is called the group interaction intensity, and the parameter m is called the pairwise interaction intensity. Note that node i only produces links if it is active, thus forming an instantaneous network G_t. At the end of time step, the existing edges in network G_t are removed.

2.2. Epidemic spreading

The classical susceptible–infected–susceptible (SIS) model was utilized to simulate epidemic spreading processes. In the model, individuals can be either susceptible (S) or infected (I). During each time step, susceptible individuals become infected at a rate of λ when they contact with infected

individuals, and infected individuals recover to susceptible at a rate of μ.

Integrating the spreading process with the network evolution allows for a more accurate representation of epidemic spreading. Theoretical estimation of the epidemic threshold and size can be derived as follows.[13] At a mean-field level, the population engaged in pairwise interactions at time t can be obtained as

$$\begin{aligned}\frac{\mathrm{d}I^t_{\mathrm{A},a}}{\mathrm{d}t} =& -\mu I^t_{\mathrm{A},a} + \lambda p N_a a m \int \mathrm{d}a' \frac{I^t_{\mathrm{A},a'} + I^t_{\mathrm{B},a'}}{N} \\ &+ \lambda p N_a m \int \mathrm{d}a' \frac{I^t_{\mathrm{A},a'}}{N} + \lambda p N_a (s-1) \int \mathrm{d}a' a' \frac{I^t_{\mathrm{B},a'}}{N} \\ &+ \lambda p N_a \int \mathrm{d}a' a' \frac{(1-p)N_{a'}}{N} (s-1) \int \mathrm{d}a'' a'' \\ &\times \frac{I^t_{\mathrm{A},a''} + I^t_{\mathrm{B},a''}}{N} (s-2), \end{aligned} \tag{1}$$

where the first term on the right-hand side represents the recovery of nodes with activity a, the second term signifies the probability that susceptible nodes with activity a of type A become active and get infected after contact with infected nodes of any activity level (hence, the integration over a'). The third term represents the susceptible nodes with activity a of type A that can be selected and infected by an active infected node with any activity level (hence, the integration over a'). Similarly, the fourth term denotes the susceptible nodes with activity a of type B that can be chosen and infected by an active infected node with any activity level (hence, the integration over a'). Finally, the last term describes the scenario where a susceptible node with activity a is selected by a susceptible node with activity a' of type B, which then becomes active (with probability at $a'\Delta t$) and creates a simplex that includes an infectious node with activity a''.

The number of population with group interaction at time t is given by

$$\begin{aligned}\frac{\mathrm{d}I^t_{\mathrm{B},a}}{\mathrm{d}t} =& -\mu I^t_{\mathrm{B},a} + \lambda (1-p) N_a a (s-1) \int \mathrm{d}a' \frac{I^t_{\mathrm{A},a'} + I^t_{\mathrm{B},a'}}{N} \\ &+ \lambda (1-p) N_a m \int \mathrm{d}a' \frac{I^t_{\mathrm{A},a'}}{N} \\ &+ \lambda (1-p) N_a (s-1) \int \mathrm{d}a' a' \frac{I^t_{\mathrm{B},a'}}{N} \\ &+ \lambda (1-p) N_a \int \mathrm{d}a' a' \frac{(1-p)N_{a'}}{N} (s-1) \int \mathrm{d}a'' a'' \\ &\times \frac{I^t_{\mathrm{A},a''} + I^t_{\mathrm{B},a''}}{N} (s-2). \end{aligned} \tag{2}$$

Accordingly, the total number of infections at time step t can be obtained from

$$I^t_a = I^t_{\mathrm{A},a'} + I^t_{\mathrm{B},a'}. \tag{3}$$

By integrating a in Eq. (3), we obtain

$$\begin{aligned}\mathrm{d}I^t =& -\mu I^t + \lambda \langle a \rangle [pm + (1-p)(s-1)^2] I^t + \lambda m \theta^t_{\mathrm{A}} \\ &+ \lambda (s-1) \theta^t_{\mathrm{B}}, \end{aligned} \tag{4}$$

where

$$\theta^t_{\mathrm{A}} = \int I^t_{a',A} a' \,\mathrm{d}a', \quad \theta^t_{\mathrm{B}} = \int I^t_{a',B} a' \,\mathrm{d}a'.$$

Multiplying both sides of Eq. (1) as well as Eq. (2) by a, and then integrating a, we obtain

$$\begin{aligned}\mathrm{d}\theta^t_{\mathrm{A}} =& -\mu \theta^t_{\mathrm{A}} + \lambda pm \langle a^2 \rangle I^t + \lambda pm \langle a \rangle \theta^t_{\mathrm{A}} + \lambda p (s-1) \langle a \rangle \theta^t_{\mathrm{B}} \\ &+ \lambda p (1-p)(s-1)(s-2) \langle a \rangle^2 I^t, \end{aligned} \tag{5}$$

$$\begin{aligned}\mathrm{d}\theta^t_{\mathrm{B}} =& -\mu \theta^t_{\mathrm{B}} + \lambda (1-p)(s-1) \langle a^2 \rangle I^t + \lambda (1-p) m \langle a \rangle \theta^t_{\mathrm{A}} \\ &+ \lambda (1-p)(s-1) \langle a \rangle \theta^t_{\mathrm{B}} + \lambda (1-p)^2 (s-1)(s-2) \langle a \rangle^2 I^t. \end{aligned} \tag{6}$$

When $m = s-1$, the Jacobian matrix J of this set of linear differential equations (4)–(6) takes the form of

$$\begin{bmatrix} \kappa_{11} & pm & pm \\ \kappa_{21} & -\mu + \lambda pm \langle a \rangle & \lambda pm \langle a \rangle \\ \kappa_{31} & \lambda (1-p) m \langle a \rangle & -\mu + \lambda (1-p) m \langle a \rangle \end{bmatrix}. \tag{7}$$

with

$$\begin{aligned} \kappa_{11} &= -\mu + \lambda [pm + (1-p)m^2] \langle a \rangle, \\ \kappa_{21} &= \lambda pm \langle a^2 \rangle + \lambda p (1-p) m (m-1) \langle a \rangle^2, \\ \kappa_{31} &= \lambda (1-p) m \langle a^2 \rangle + \lambda (1-p)^2 m (m-1) \langle a \rangle^2. \end{aligned}$$

The disease will be able to spread only when the largest eigenvalue of the Jacobian matrix J of the system (7) is larger than zero. This yields the epidemic threshold

$$\frac{\lambda}{\mu} = \frac{2}{m \langle a \rangle l + m \sqrt{\langle a \rangle^2 l^2 - 4(\langle a \rangle^2 - \langle a^2 \rangle)}}, \tag{8}$$

where

$$l = [1 + p + (1-p)m].$$

3. Simulation results and discussion

In this section, we analyze the influence of various social interactions on the spread of epidemic. Numerical simulations are carried out using the following parameters: population size $N = 2000$, time step $\Delta t = 1$, recovery rate $\mu = 0.01$, $0.01 \leqslant a \leqslant 1$, $\gamma_a = 2.1$, $m = 3$, and $s = 4$. The initial fraction of infected nodes is set to 0.01. Simulations are performed for $T = 10000$ steps, and the average covers the final 1000 steps. Each presented result is an average of 100 independent experiments conducted through Monte Carlo simulations.

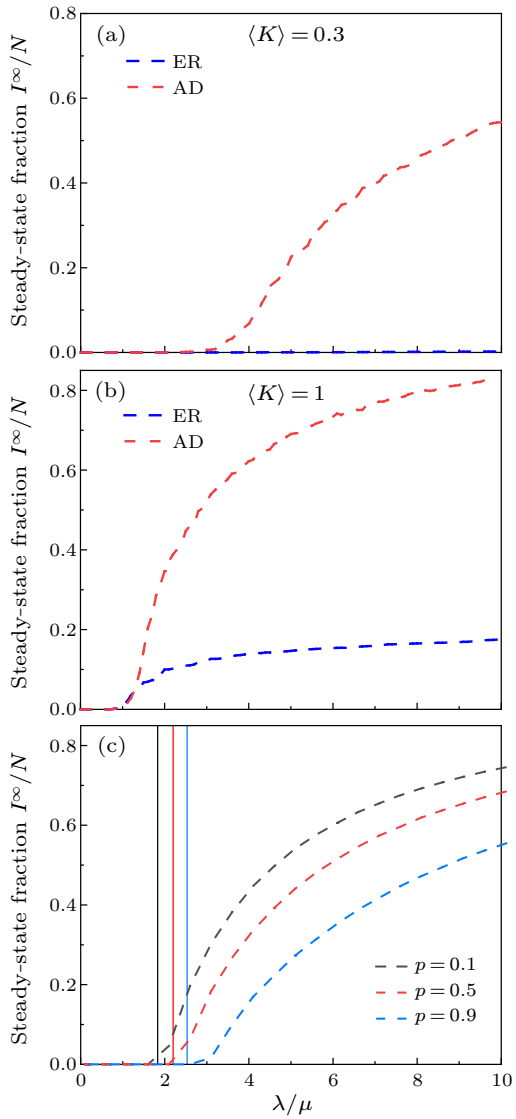


Fig. 3. The relationship between the steady-state fraction of infected individuals I^∞/N and λ/μ for Erdos–Renyi (ER) random network and activity-driven (AD) network with the same average degree of $\langle K\rangle = 0.3$ (a), and $\langle K\rangle = 1.0$ (b). (c) The relationship between the steady-state fraction of infected individuals I^∞/N, λ/μ and the pairwise interaction proportion p, with $p = 0.1$ (black), 0.5 (red), 0.9 (blue). The vertical lines on the plot represent the theoretical thresholds calculated with Eq. (8).

Figures 3(a) and 3(b) display the relationship between the steady-state fraction of infected individuals I^∞/N and epidemic parameter λ/μ for static Erdos–Renyi (ER) random network and activity-driven (AD) network with the same average degree of $\langle K\rangle = 0.3$, and $\langle K\rangle = 1.0$, respectively. One can see that, when the average degree is low [Fig. 3(a)], disease will spread in the AD network when $\lambda/\mu > 2.5$, while it will disappear in the ER network. This is due to the fact that the nodes are not well-connected when the links are very sparse, so that the epidemic spreading is local and limited. In the AD network, active nodes and the links appear at different times, providing a passageway for the virus to spread in the system. When the average degree is high [Fig. 3(b)], the epidemic will spread in both static ER networks and dynamic AD networks. Although both networks show similar threshold of epidemic spreading, the steady-state fraction of infected individuals of the AD network is much higher than the ER network. The different behavior of static ER networks and dynamic AD networks shows the importance of investigating the effect of time-dependent networks on the spreading of epidemics.

Figure 3(c) further shows the relationship between the steady-state fraction of infected individuals I^∞/N and epidemic parameter λ/μ for different value of pairwise interaction proportion p. The results show that the epidemic size increases with λ/μ. With a larger pairwise interaction proportion, a higher threshold and a smaller size of epidemic will be observed. This is due to the fact that a decrease of group interactions means a reduction in social gatherings, consequently limiting the spread of the epidemic.

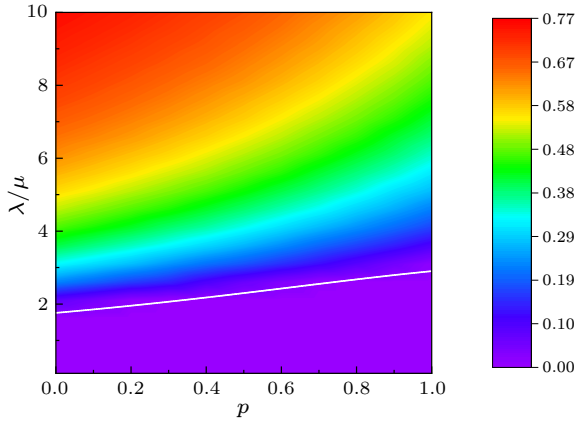


Fig. 4. The relationship between the steady-state fraction of infected individuals I^∞/N (color coded), λ/μ and the pairwise interaction proportion p. The white solid line corresponds to the theoretical threshold calculated using Eq. (8).

Figure 4 illustrates the variation of steady-state fraction of infected individuals I^∞/N with epidemic parameter λ/μ and pairwise interaction proportion p. One can see that, for different p, the scale of infection increases with λ/μ. Meanwhile, the epidemic threshold increases with p. The simulation results agree well with the result of theoretical thresholds. As p increases, a higher value of λ/μ is needed to attain a given steady-state fraction of infection. This indicates that as the pairwise interaction proportion increases, it becomes more difficult for the epidemic to spread. Conversely, a higher prevalence of individuals with group interactions increases the likelihood of epidemic outbreak.

Figure 5 shows the relationship between the steady-state fraction of infected individuals I^∞/N and the epidemic parameter λ/μ, for various values of pairwise interaction proportion p and group interaction parameter s. Note that $(s-1)$ represents the group social intensity. One can see that, for all values of p and s, the infection density increases with λ/μ. Increase the pairwise interactions proportion p results in a higher epidemic threshold and a reduction in the scale of the epidemic.

Figures 5(a)–5(c) show that, as the pairwise interaction proportion p increases, the threshold variation value decreases. For $p = 0.2$, the threshold range changes from 1.4 to 3.2, and for $p = 0.8$, the threshold range changes from 1.8 to 2.8. Furthermore, as the pairwise interaction proportion p increases, the infection size variation value gradually decreases. For $p = 0.2$, the proportion of infected nodes decreases from 0.83 to 0.57, and when $p = 0.8$, the proportion of infected nodes decreases to 0.59.

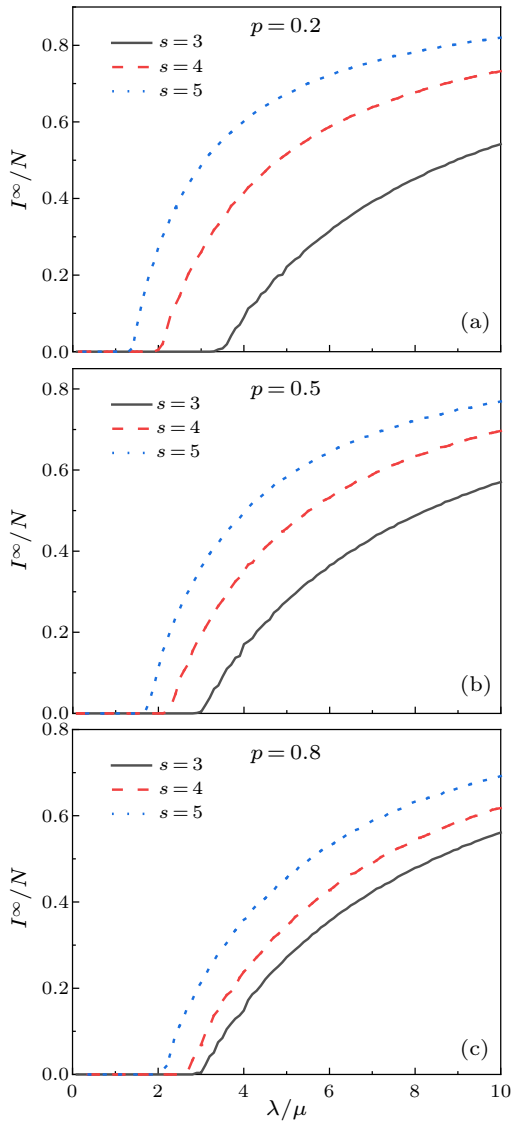


Fig. 5. The steady-state fraction of infected individuals I^{∞}/N as a function of λ/μ with different values of group social parameter s for $p = 0.2$ (a), $p = 0.5$ (b), and $p = 0.8$ (c).

We further investigate the relationship between the steady-state fraction of infected A-type/B-type individuals and the epidemic parameter λ/μ. Figure 6 shows the steady-state fraction of infected individuals I^{∞}/N as a function of pairwise interaction proportion p for different values of group interaction parameter s ($s = 3$, 4, and 5). It is evident that, the size of infection decreases when the level of group social intensity is greater than or equal to the pairwise social intensity (e.g., when $s = 4$ and $s = 3$) as the pairwise interaction proportion p increases. On the other hand, when the level of group social intensity is less than the pairwise social intensity (e.g., $s = 3$), the size of infection generally increases as p increases. This phenomenon can be attributed to an increase in the number of individuals engaged in pairwise interactions, indicating an increase in the number of socially intense individuals within the group. Consequently, this can lead to a rise in the overall number of contacts within the network and, subsequently, an increase in the size of the infection.

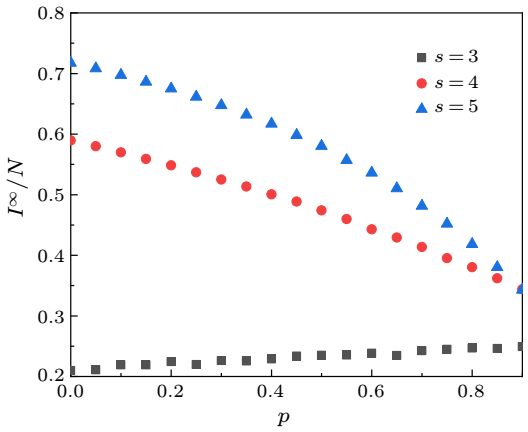


Fig. 6. The relationship between the steady-state fraction of infected individuals I^{∞}/N and the pairwise interaction proportion (p) under different group interaction parameter $s = 3$ (square), 4 (circle), 5 (triangle). Here we fix $\lambda = 0.05$.

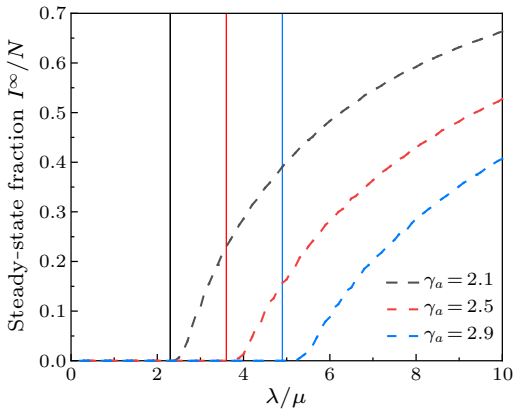


Fig. 7. The relationship between the steady-state fraction of infected individuals I^{∞}/N, and the λ/μ ratio under different exponents γ_a. The vertical lines indicate the theoretical thresholds calculated with Eq. (8) for three different values: $\gamma_a = 2.1$ (black), $\gamma_a = 2.5$ (red), $\gamma_a = 2.9$ (blue), and the pairwise interaction proportion $p = 0.7$.

Figure 7 presents the epidemic size against epidemic parameter λ/μ for various exponents γ_a. It is evident that, irrespective of the value of γ_a, the epidemic size consistently increases with higher values of λ/μ. A smaller γ_a value signifies a more heterogeneous activity distribution,[26] indicating a greater degree of heterogeneity in the network. Consequently, larger epidemic sizes are observed at the same λ/μ when the activity distribution is more heterogeneous. This phenomenon can be attributed to the presence of hub nodes in the social network. Infection among hub nodes facilitates the rapid spread

of the epidemic throughout the network. Conversely, reducing the heterogeneity of the network can restrict the spread of an epidemic.

4. Conclusion

In summary, the influence of pairwise and group social interactions on the spread of epidemics is explored in activity-driven time-dependent social networks. Higher-order simplicial structures are adopted to describe group interactions. Mean-field approach is extended to derive the epidemic threshold for the activity-epidemic model theoretically. Monte Carlo simulations are carried out to verify the theoretical results.

The research yields several key findings. First, when the group social intensity is equal to the pairwise social intensity, as the pairwise interaction proportion increases, the epidemic threshold increases and the infection scale decreases. Second, regardless of the value of the pairwise interaction proportion, as group social intensity decreases, the epidemic threshold increases and the infection scale decreases. Third, when the level of group social intensity is greater than or equal to the pairwise social intensity, the infection scale tends to decrease as the pairwise interaction proportion increases. Conversely, when the level of group social intensity is less than the pairwise social intensity, the size of infection tends to increase as the pairwise interaction proportion increases. Furthermore, a weak heterogeneous distribution of activities can elevate the threshold of epidemic and reduce the scale of infection.

These findings emphasize the significance of group interactions in the spread of epidemics. The results are helpful for designs of epidemic control strategies in long-term process of fighting against COVID viruses.

Acknowledgments

This work was supported by the National Natural Science Foundation of China (Grant No. 12072340), the China Postdoctoral Science Foundation (Grant No. 2022M720727), and the Jiangsu Funding Program for Excellent Postdoctoral Talent (Grant No. 2022ZB130).

References

[1] Chen J J, Hu M B and Wu Y H 2022 *Chaos Soliton Fract.* **161** 112348
[2] Zeng L, Zeng Y Q and Tang M 2022 *Phys. Rev. Res.* **4** 033209
[3] Yang H X and Wang B H 2016 *Physica A* **443** 86
[4] Fu C, Liu X Y and Yang J 2019 *IEEE Trans. Depend. Secure Comput.* **16** 693
[5] Vega-Oliveros D A, Costa L D and Rodrigues F A 2020 *Commun. Nonlinear Sci.* **83** 105094
[6] Xu S H, Lu W L and Zhan Z X 2012 *IEEE Trans. Depend. Secure Comput.* **9** 30
[7] Ren J G and Xu Y H 2018 *Appl. Math. Model.* **59** 86
[8] Boguna M, Castellano C and Pastor-Satorras R 2013 *Phys. Rev. Lett.* **111** 068701
[9] Vespignani A 2011 *Nat. Phys.* **8** 32
[10] Valdano E, Poletto C and Colizza V 2015 *Eur. Phys. J. B* **88** 341
[11] Perra N, Goncalves B and Pastor-Satorras R 2012 *Sci. Rep.* **2** 469
[12] Wang B, Xie Z Y and Han Y X 2021 *Phys. Rev. E* **104** 044307
[13] Hou Y X, Lu Y K and Dong Y T 2023 *Appl. Math. Comput.* **446** 127850
[14] Li Z C and Tang J H 2017 *IEEE Trans. Image Process.* **26** 276
[15] Li Z C, Tang J H and Mei T 2019 *IEEE Trans. Pattern Anal.* **41** 2070
[16] Centola D 2010 *Science* **329** 1194
[17] Patania A, Petri G and Vaccarino F 2017 *EPJ Data Sci.* **6** 18
[18] Wang H, Ma C and Chen H S 2022 *Nat. Commun.* **13** 3043
[19] Zhao X M, Yu H T and Li S M 2022 *Physica A* **606** 128073
[20] Fan J F, Yin Q and Xia C Y 2022 *Proc. R. Soc. A* **478** 20220059
[21] Iacopini I, Petri G and Barrat A 2019 *Nat. Commun.* **10** 2485
[22] Petri G and Barrat A 2018 *Phys. Rev. Lett.* **121** 228301
[23] Long E, Patterson S and Maxwell K 2022 *J. Epidemiol. Commun. Health* **76** 128
[24] Calbi M, Langiulli N and Ferroni F 2021 *Sci. Rep.* **11** 2601
[25] Buckee C, Noor A and Sattenspiel L 2021 *Nature* **595** 205
[26] Wang H, Zhang H F and Zhu P C 2022 *Chaos* **32** 083110